

A consistent collinear triad approximation for operational wave models



J.E. Salmon^{a,*}, P.B. Smit^b, T.T. Janssen^b, L.H. Holthuijsen^a

^aFaculty of Civil Engineering and Geosciences, Delft University of Technology, The Netherlands

^bNorthWest Research Associates, El Granada, CA, USA

ARTICLE INFO

Article history:

Received 13 February 2016

Revised 22 June 2016

Accepted 26 June 2016

Available online 27 June 2016

Keywords:

Wave-wave interactions

Wave model

Surf zone

Wave propagation

Coastal zone

Coastal systems

ABSTRACT

In shallow water, the spectral evolution associated with energy transfers due to three-wave (or triad) interactions is important for the prediction of nearshore wave propagation and wave-driven dynamics. The numerical evaluation of these nonlinear interactions involves the evaluation of a weighted convolution integral in both frequency and directional space for each frequency-direction component in the wave field. For reasons of efficiency, operational wave models often rely on a so-called collinear approximation that assumes that energy is only exchanged between wave components travelling in the same direction (collinear propagation) to eliminate the directional convolution. In this work, we show that the collinear approximation as presently implemented in operational models is inconsistent. This causes energy transfers to become unbounded in the limit of unidirectional waves (narrow aperture), and results in the underestimation of energy transfers in short-crested wave conditions. We propose a modification to the collinear approximation to remove this inconsistency and to make it physically more realistic. Through comparison with laboratory observations and results from Monte Carlo simulations, we demonstrate that the proposed modified collinear model is consistent, remains bounded, smoothly converges to the unidirectional limit, and is numerically more robust. Our results show that the modifications proposed here result in a consistent collinear approximation, which remains bounded and can provide an efficient approximation to model nonlinear triad effects in operational wave models.

© 2016 Elsevier Ltd. All rights reserved.

1. Introduction

The evolution of ocean waves due to three-wave (or triad) interactions near the coast and in shallow water is important for the prediction of nearshore wave characteristics (see e.g. Herbers et al., 2000) and wave-driven dynamics (see e.g. Hoefel and Elgar, 2003). In deep water, these interactions are generally off-resonant and the nonlinear evolution is governed by higher-order resonances (Hasselmann, 1962). In contrast, near the coast, due to reduced water depth, these three-wave interactions approach resonance and can drive $O(1)$ energy transfers on length scales of $O(10)$ wavelengths (e.g. Janssen et al., 2006). In particular, in the surf zone, the evolution of the wave spectrum is almost entirely dictated by the balance between nonlinear triad interactions and depth-induced breaking (e.g. Kaihatu and Kirby, 1995; Herbers et al., 2000; Smit et al., 2014). Accounting for these effects in operational wave models for coastal wave propagation (e.g. Tolman, 1990; Komen et al., 1994; Booij et al., 1999) is therefore important.

Operational wave models describe the spatial 2D evolution of the directional wave spectrum $E(\sigma, \theta; \mathbf{x}, t)$ through geographical space $\mathbf{x} = (x, y)$, and through frequency σ and directional space θ , by solving a wave action balance equation of the form (e.g. WAMDI Group, 1988):

$$\frac{\partial N}{\partial t} + \frac{\partial c_{g,x} N}{\partial x} + \frac{\partial c_{g,y} N}{\partial y} + \frac{\partial c_{\sigma} N}{\partial \sigma} + \frac{\partial c_{\theta} N}{\partial \theta} = \frac{S}{\sigma}. \quad (1)$$

Here, $N(\sigma, \theta; \mathbf{x}, t) = E/\sigma$ is the wave action density, $\sigma = 2\pi f$ is the radian frequency, $c_{g,x}$, $c_{g,y}$, c_{σ} , c_{θ} denote transport velocities in geographical, frequency and directional space, respectively, and S represents the source terms that account for non-conservative and nonlinear processes, including triad interactions. The difficulty with incorporating three-wave nonlinearity is that these interactions will result in the development of high-order correlations for which a separate transport equation should be evaluated, and some closure approximation invoked (e.g. Eldeberky, 1996; Becq-Girard et al., 1999; Herbers et al., 2003; Janssen, 2006). Because of the inherent complexity of the problem and for reasons of efficiency, much effort has gone into developing efficient approximations for the evolution of the unidirectional energy density spec-

* Corresponding author.

E-mail address: salmonjames@gmail.com (J.E. Salmon).

trum $E(\sigma; \mathbf{x}, t)$ (e.g. Eldeberky, 1996; Becq-Girard et al., 1999; Toledo and Agnon, 2012). In this context, one of the first – and perhaps most widely used – of these approximations is the Lumped Triad Approximation (LTA; Eldeberky, 1996). This efficient approximation, which amongst numerous other simplifications (see e.g. Becq-Girard et al., 1999), accounts only for self-self interactions and takes the form

$$S_{nl3}^{1D}(\sigma_1) \propto (W_1)^2 [(E_2)^2 - 2E_1E_2] - 2(W_3)^2 [(E_1)^2 - 2E_1E_3] \quad (2)$$

where $W_i = W(\sigma_i, x)$ is an interaction coefficient (given by Madsen and Sørensen, 1993; their Eq. 5.4) and $E_i = E(\sigma_i)$ with $\sigma_1 = \sigma$, $\sigma_2 = \sigma/2$ and $\sigma_3 = 2\sigma$. For brevity, the dependence on x (or \mathbf{x}) and t is implied in the spectral quantities. To apply this unidirectional self-self formulation in a fully directional model, Booij et al. (1999) proposed to use Eq. (2) along each spectral direction. This is achieved by simply replacing each occurrence of E_i in Eq. (2) with its directional counterpart $E_i^1 = E(\sigma_i, \theta_1)$ to obtain the directional source term

$$S_{nl3}(\sigma_1, \theta_1) \propto (W_1)^2 [(E_2^1)^2 - 2E_1^1E_2^1] - 2(W_3)^2 [(E_1^1)^2 - 2E_1^1E_3^1]. \quad (3)$$

The source term defined in Eq. (3) is what is known as the collinear approximation which we will refer to as the Original Collinear Approximation (OCA). In this approximation, directional components are completely isolated so that each discrete direction is treated as an independent unidirectional wave field. The assumption that energy transfers predominantly occur between (almost) collinear waves is probably reasonable for harmonic generation and transfer of energy to shorter waves in wave fields propagating over a relatively uniform beach. However, over complicated topography, where energy transfers between waves at significant angles may be important (Toledo, 2013; Groeneweg et al., 2015), this approximation should generally be used with care. Moreover, the collinear approximation is not at all suited for modelling infragravity wave generation for which full directionality would have to be retained (Herbers et al., 1995).

Even though directionally-coupled models are available (e.g. the fully directional SPB model; Becq et al., 1998), the collinear approximation is still the most widely applied triad model (for instance in e.g. WAVEWATCH III, SWAN, TOMAWAC), principally because the numerical evaluation of these less restrictive models is prohibitively expensive for routine operational use. Despite its continued use, the performance of the directional version of the LTA is highly unsatisfactory, which is often ascribed to the shortcomings of the underlying LTA model. As a consequence, efforts towards the improvement of the OCA have focused on improving the underlying LTA approximation (see e.g. Booij et al., 2009).

Although the LTA model is undoubtedly a crude approximation, the principal source of the errors in the OCA is not due to the LTA. Instead, it results from the directional decoupling as applied in the OCA. For instance, from Eq. (3) it can be shown that the OCA predicts unbounded energy transfers in the limit of unidirectional waves, and generally underestimates nonlinear transfers in short-crested seas. To illustrate this numerically, we consider energy transfers predicted by $S_{nl3}(\sigma, \theta)$ (as implemented in SWAN) for a directional wave spectrum of the form $E(\sigma, \theta) = D(\theta)E(\sigma)$. In the simulations, we increasingly reduce the aperture of the directional distribution $D(\theta)$, while maintaining the same frequency spectrum $E(\sigma) = \int E(\sigma, \theta)d\theta$. From these simulations (see Fig. 1), we see that the energy transfers as predicted by the OCA become excessively large as the directional width is reduced. In fact these transfers greatly exceed the energy transfers predicted by the unidirectional triad model of Eldeberky (1996) on which the SWAN collinear model is based, and to which it should reduce to if the collinear model is consistent.

Clearly, the excessive energy transfers for narrow directional apertures indicates that the collinear approximation fails to reduce to the unidirectional limit. This inconsistency is the principal motivation for the present study. To identify the source of the error, we revisit the formulation of the collinear approximation as used in various models and provide a more consistent formulation that removes the unrealistic sensitivity to directional aperture, while retaining similar efficiency gains (Section 2). By no means do we argue that the collinear approximation, even in a more consistent form, represents a complete description of the three-wave interactions. However, we acknowledge that approximations for increasing efficiency are a reality for many operational applications and our objective here is to improve the collinear approximation to ensure it is at the very least internally consistent to improve its potential for operational use.

To show the differences between the original and proposed approximation, we calibrate and validate both collinear models using laboratory data, and with Monte Carlo simulations with a deterministic model (Section 3 and 4). We discuss and summarize our principal results and their implications in Section 5 and 6.

2. Collinear triad approximations

In order to identify the source of the inconsistency in the OCA, and derive an improved version of the collinear approximation, the Consistent Collinear Approximation (CCA), we consider the source term for energy transfers due to triad interactions for weakly nonlinear waves over slowly varying bathymetry. This can be written as (e.g. Eldeberky, 1996; Becq et al., 1998; Smit and Janssen, 2016)

$$S_{nl3}(\sigma_1, \theta_1) = c_{g,1} \int_0^{2\pi} \int_{-\infty}^{\infty} W_{2,1-2}^{2,1-2} \text{Im}\{B_{2,1-2}^{2,1-2}\} d\sigma_2 d\theta_2 \quad (4)$$

where W is a real coupling coefficient, B denotes the bispectrum and $\text{Im}\{\dots\}$ denotes the imaginary part of the argument. The shorthand notation $W_{2,1-2}^{2,1-2}$ (and for B , E etc.) relates to $W(\sigma_2, \sigma_1 - \sigma_2, \theta_2, \theta_1 - \theta_2)$ where the subscript and superscript denote the frequency and directional components involved, respectively. Eq. (4) gives the complete source term for a WKB approximation of weakly nonlinear waves. In order to arrive at a collinear approximation we need to introduce a series of assumptions, and we will step through them systematically. As a first step, all the interaction coefficients are replaced by their unidirectional equivalents (i.e. $W_{2,1-2}^{2,1-2} \rightarrow W_{2,1-2}^{1,1} \equiv W_{2,1-2}$) and the bispectrum is expressed in terms of local products of the spectral components while making use of its symmetries, so that S_{nl3} can be written as

$$S_{nl3}(\sigma_1, \theta_1) = 2c_{g,1} \left[\int_0^{\sigma_1} W_{2,1-2} \overline{B_{2,1-2}^1} d\sigma_2 - 2 \int_0^{\infty} W_{2,1} \overline{B_{2,1}^1} d\sigma_2 \right] \quad (5)$$

where the first and second integrals represent contributions due to the sum and difference interactions, respectively, and

$$\overline{B_{2,1-2}^1} = \Phi_{2,1-2}^1 \int_0^{2\pi} Q_{2,1-2}^{2,1-2} d\theta_2. \quad (6)$$

Here $\Phi_{2,1-2}^1 = \Phi(\sigma_2, \sigma_1 - \sigma_2, \theta_1)$ is an (empirical) factor that approximately accounts for the closure approximation implied and the development of the bispectrum towards resonance for collinear shallow waves (see e.g. Becq-Girard et al., 1999), and

$$Q_{2,1-2}^{2,1-2} = [W_{2,1-2} E_2^2 E_{1-2}^{1-2} - E_1^1 (W_{1,-2} E_2^2 + W_{1,2-1} E_{1-2}^{1-2})]. \quad (7)$$

Equivalent expressions for the difference contribution are achieved by replacing the subscript and superscript pairs. The expression of the bispectrum in terms of an algebraic relation to products of local energies is possible by introducing a quasi-normal

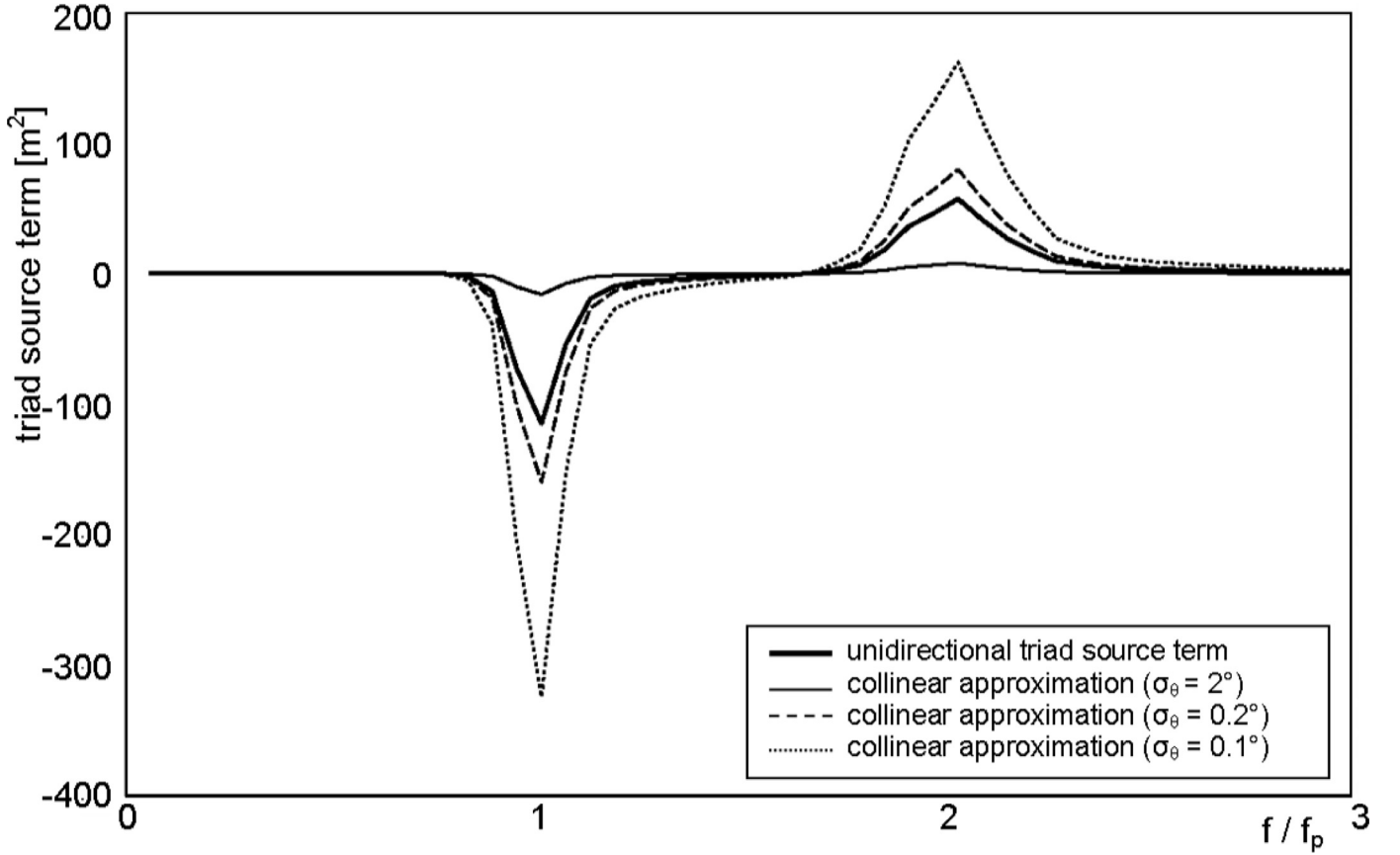


Fig. 1. Energy transfers due to nonlinear triad interactions for a wave field with a JONSWAP spectrum ($H_{m0} = 5$ m and $T_p = 12$ s) in 5 m water depth for varying directional widths as computed by the OCA implementation in SWAN (see Booij et al., 1999). As the directional width is reduced, energy transfers greatly exceed the transfers predicted by the unidirectional triad model of Eldeberky (1996; thick solid line) on which the OCA model is based, and to which it should – in theory – reduce to. The fact that it does not suggests that there is an inconsistency in the collinear approximation.

closure approximation for the nonlinear hierarchy and assuming that three-wave correlations can be expressed in terms of the products of local spectral components (see Herbers et al., 2003; Janssen, 2006). Although all the assumptions to approximate the nonlinear term can be questioned independently, we will assume here that they are reasonable for the intended range of application of the collinear approximation.

From here, the final step towards the collinear approximation is to replace all the spectral components by the directional components, simply drop the directional integration, and add a calibration constant for tuning. The Original Collinear Approximation (OCA) can then be written as

$$\overline{B_{2,1-2}^1} \approx \overline{B_{2,1-2}^{1,(OCA)}} = \alpha \Phi_{2,1-2}^1 Q_{2,1-2}^1 \quad (8)$$

with

$$Q_{2,1-2}^1 = [W_{2,1-2} E_2^1 E_{1-2}^1 - E_1^1 (W_{1,-2} E_2^1 + W_{1,2-1} E_{1-2}^1)] \quad (9)$$

and where α is a (dimensional) calibration constant. Effectively, with these approximations each direction is considered in isolation as if it was a unidirectional wave field and energy is only exchanged between collinear components. From the series of approximations, it is this last step which introduces the inconsistency that causes the erratic behavior for narrow-aperture waves (see Fig. 1).

By simply dropping the directional integration, the effects of directional width are effectively (but implicitly) moved to the calibration coefficient, which thus becomes strongly dependent on the directional aperture of the wave field. The consequence of this is that, once calibrated, energy transfers become exaggerated when applied to wave fields with narrower apertures than for which it

was calibrated. This can be readily seen if we consider the special case of a wave field with directional aperture $\Delta\theta$, and a uniform distribution of wave energy in directional space, such that $E(\sigma, \theta) = E(\sigma)/\Delta\theta$ for $\theta \in \Delta\theta$ (and 0 elsewhere). For this case, due to the omission of the directional integral, without making any provisions to ensure dimensional consistency, we have

$$\overline{B_{2,1-2}^{1,(OCA)}} = \frac{\alpha}{\Delta\theta} \overline{B_{2,1-2}^1} \quad (10)$$

This shows that for a given, and fixed, value of the calibration coefficient α , the dropping of the directional integration introduces a strong dependency on the directional aperture $\Delta\theta$ and in the limit of $\Delta\theta \rightarrow 0$ the result becomes unbounded. This is what causes the erratic behavior for the energy transfers in general and unrealistic amplification of energy transfers for small aperture wave fields specifically, as seen in Fig. 1.

2.1. A consistent collinear approximation (CCA)

Although the collinear approximation relies on a number of assumptions to simplify the numerical evaluation, it is principally the dropping of the directional integration that introduces an inconsistency and limits the potential of the collinear approximation in operational wave models. To maintain a similar level of efficiency, while bypassing this inconsistency, we propose a slight modification of the collinear terms, which can be written as

$$\overline{B_{2,1-2}^{1,(CCA)}} = \alpha \Phi_{2,1-2}^1 \overline{Q_{2,1-2}^1} \quad (11)$$

where

$$\overline{Q_{2,1-2}^1} = \frac{1}{2} \left(W_{2,1-2} \overline{E_2^1 E_{1-2}^1} - \overline{E_1^1} \{ W_{1,-2} E_2^1 + W_{1,2-1} E_{1-2}^1 \} \right) + \frac{1}{2} \left(W_{2,1-2} E_2^1 \overline{E_{1-2}^1} - E_1^1 \{ W_{1,-2} \overline{E_2^1} + W_{1,2-1} \overline{E_{1-2}^1} \} \right) \quad (12)$$

in which

$$\overline{E_i^j} = \int_{\theta_j - p_\theta/2}^{\theta_j + p_\theta/2} E(\sigma_i, \theta) d\theta \quad (13)$$

and where p_θ is a tuning parameter which determines how close the approximation mimics a unidirectional model. Effectively thus, in this approximation, which we refer to as the Consistent Collinear Approximation (CCA), instead of simply dropping the directional convolution integral (see Eq. 4) we assume that

$$\int_0^{2\pi} E_2^2 E_{1-2}^2 d\theta_2 \propto \frac{1}{2} \left[\overline{E_2^1 E_{1-2}^1} + E_2^1 \overline{E_{1-2}^1} \right] \quad (14)$$

and absorb the dimensionless constant of proportionality into the calibration factor α . By rewriting the collinear approximation in this way, we prevent the inconsistency and potential singularity as present in the original formulation. Moreover, since $\overline{E_2^1} \leq \int_0^{2\pi} E_2^1 d\theta = E_2$ it follows that $\frac{1}{2} \int_0^{2\pi} [\overline{E_2^1 E_{1-2}^1} + E_2^1 \overline{E_{1-2}^1}] d\theta \leq E_2 E_{1-2}$ so that the directionally-integrated energy transfers are always less than or equal to the transfers in an equivalent unidirectional wave field. The latter is internally consistent with the underlying premise that the collinear interactions are closest to resonance and are the most efficient contributors to the nonlinear transfers. In fact, with $p_\theta = 2\pi$, the integrated energy transfer becomes

$$S_{nl3}(\sigma) = \int_0^{2\pi} S_{nl3}(\sigma, \theta) d\theta = S_{nl3}^{1D}(\sigma) \quad \text{with } p_\theta = 2\pi$$

In this sense, the parameter p_θ is an independent calibration parameter, such that if the magnitude of p_θ is reduced (and thus the integration aperture in the interaction term), the strength of the interactions in wide-aperture wave fields is suppressed, consistent with what is typically observed. Although the CCA (Eq. 11) does require an additional directional integral (compared to the OCA), its efficiency is similar to the OCA since it reduces the full convolution to a simple one-dimensional integral and a multiplication, while still reproducing the qualitative features of Eq. (8).

For a complete model, we would still need to introduce suitable approximations for the closure factor $\Phi_{2,1-2}^1$, which in itself has not been resolved in the literature (see, for example, Orszag, 1974; Janssen, 2006 for an overview) and is outside the scope of this work. Since our primary goal is to resolve the directional sensitivity issue in the OCA, and to allow a direct comparison between the models, we will continue to use the closure assumption and other simplifications as implied by the LTA. However, to emphasize that the collinear approximation, and the improvement proposed in this work is in essence an approximation layer on top of an underlying 1D triad model, we also implement an OCA and CCA version of the Stochastic Parametric Boussinesq (SPB) model by Becq-Girard et al. (1999). This model differs from the LTA-based collinear model in that it accounts for triad interactions between all frequency components and not just the self-self interactions. In essence, the collinear SPB implementation has the same decoupling between directional components, but includes all wave-wave interactions for each directional component individually and does not suffer from the limitations of the restriction to only self-self interactions as does the LTA. For further details regarding the two different models, we refer to Appendix A.

3. Model setup and observations

In what follows, we compare simulations with the SWAN wave model (version 40.91A) using both the Original Collinear Ap-

proximation (OCA, Eq. 8) and the Consistent Collinear Approximation (CCA, Eq. 11) for a range of different wave conditions. We couple the collinear approximations to both the LTA model (Eldeberky, 1996) and the SPB model (Becq-Girard et al. 1999). Furthermore, in the CCA, we set $p_\theta = 2\pi$ for all the numerical results, and discuss the implications of other choices for p_θ in Section 5. Model simulations are run with the dissipative source terms suggested by Zijlema et al. (2012) with the Battjes and Janssen (1978) depth-induced wave breaking model scaled with $\gamma = 0.73$ and the curvature-based stopping criteria of Zijlema and van der Westhuysen (2005) with a cap of 50 iterations.

To calibrate the models, we consider two unidirectional laboratory data sets described by Beji and Battjes (1993) and Boers (1996) with random waves (characterized by a JONSWAP spectrum at the wave maker) propagating over a barred-beach profile (see Fig. 2). The Beji and Battjes (1993) data set consists of a single wave condition with a significant wave height of $H_{m0} = 0.023$ m and a peak period of $T_p = 2.0$ s. The Boers (1996) data set consists of three wave conditions with $H_{m0} = 0.160, 0.220$ and 0.107 m and $T_p = 2.1, 2.1$ and 3.4 s, respectively. We chose these data sets as they have been used extensively for calibration in previous triad studies (see e.g. Booij et al., 1999 and van der Westhuysen, 2007). Following those studies, we approximate the unidirectional conditions with a small (but otherwise arbitrary) directional width of $\sigma_\theta = 2^\circ$ (as defined by Kuik et al., 1988) uniformly over all frequencies. Furthermore, computations are performed with frequency resolution $\Delta f = 0.05f$ and frequency range $[0.0837, 2.5]$ Hz and $[0.15, 2.0]$ Hz for the Beji and Battjes, and Boers data set, respectively. Computations include a 20° directional sector, centered about the mean wave direction with $\Delta\theta = 0.05^\circ$. Subsequently, to demonstrate the sensitivity of the collinear approximations to the directional aperture of the incident wave field, we perform simulations with varying directional widths ranging from $0.1^\circ \leq \sigma_\theta \leq 5^\circ$.

To verify the effect of the collinear approximation for directional wave fields, for which detailed observations are less readily available, we compare the collinear approximation models to Monte Carlo simulations with a second-order accurate deterministic Boussinesq model based on an angular-spectrum decomposition (Herbers and Burton, 1997). Although the interaction coefficients in the Herbers and Burton (1997) model are slightly different from those in the LTA and SPB models (which also differ), these differences are negligible compared to the effects of the collinear and closure approximations in these models. The only physical processes included in the deterministic model and the SWAN models are the triad interactions and depth-induced wave breaking dissipation (all other source terms are turned off in SWAN). Since dissipation in the deterministic model is implemented consistently with SWAN, we can ascribe any differences between the Monte Carlo simulations and the collinear approximations to the collinear approximation, and the closures implied by the LTA and SPB models.

The directional wave simulations are run over a plane beach using the same beach profile as in the laboratory setup of Smith (2004; see Fig. 3). However, instead of unidirectional incident waves, we generate directional wave conditions at the incident wave boundary. We use the laboratory setup by Smith (2004) so that we can verify the deterministic model for unidirectional wave propagation against observations for the same beach profile (not shown).

The simulations are initialized at Station 1 (see Fig. 3) with spectra identical to that measured by Smith (2004). The incident wave field consists of a TMA spectrum with $H_{m0} = 0.09$ m, $T_p = 2.5$ s and $\gamma_{TMA} = 3.3$ for Case A (broad-banded in frequency space) and $\gamma_{TMA} = 100$ for Case B (narrow-banded). For the directional distribution, we apply a $\cos^m\theta$ model uniformly to all frequencies and consider the directional widths $\sigma_\theta = 2^\circ, 4^\circ, 10^\circ, 20^\circ$ and 30° .

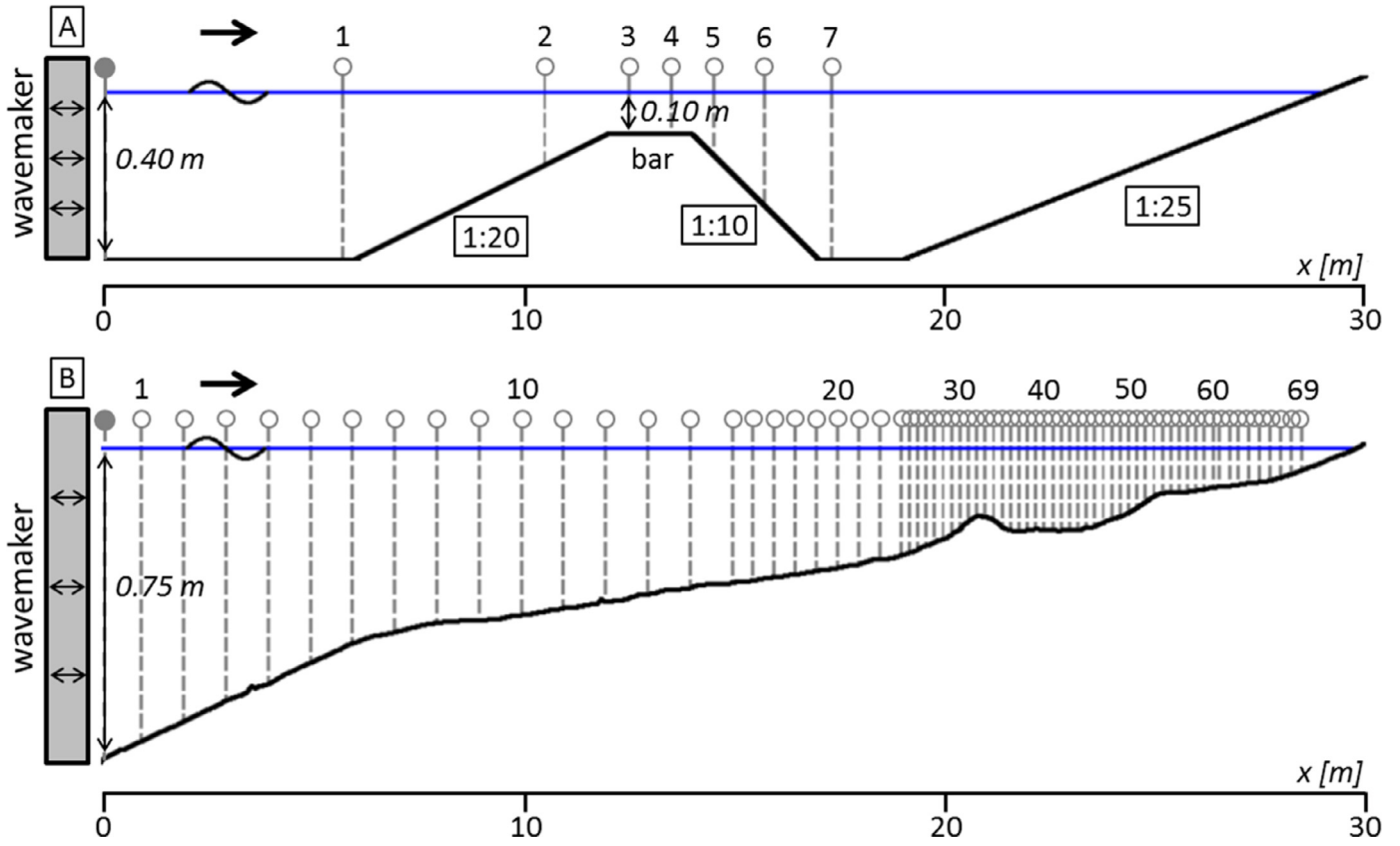


Fig. 2. Configuration of the Beji and Battjes (1993; Panel A) and Boers (1996; Panel B) laboratory flume experiments. The measurement locations are indicated by the vertical dashed lines and the location of the offshore boundary is indicated by the solid dot near the wavemaker.

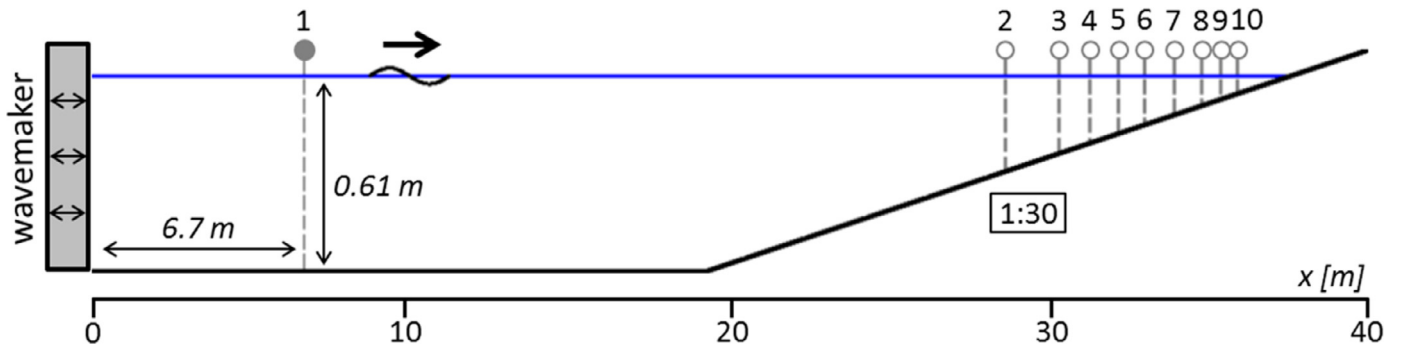


Fig. 3. Configuration of the Smith (2004) laboratory flume experiment. Annotations are as in Fig. 2.

Monte Carlo simulations with the deterministic model consist of 128 realizations with a spatial resolution $\Delta x = 0.025$ m, a lateral wavenumber array defined as $\Delta k_y[-M/2 + 1, \dots, M/2]$ with $M = 32$ and $\Delta k_y = 0.1$, and a frequency array consisting of 120 frequencies with $\Delta f = 0.025$ Hz. In what follows, we consider the deterministic model results as a proxy for observations, and compare these with SWAN computations with similar settings as before but with $\Delta f = 0.1f$ (over the range [0.2, 3.0] Hz) and $\Delta\theta = 1^\circ$ over a full circle.

4. Results

4.1. Unidirectional random waves

To calibrate α for both collinear models (OCA and CCA) and both triad closure models (LTA and SPB), α was varied over the range $0.01 \leq \alpha \leq 1.50$ with $\Delta\alpha = 0.01$. For each data set,

the scatter index, $s.i. = \sqrt{N \sum (\chi_{comp.} - \chi_{obs})^2} / \sum \chi_{obs}$ was computed where N denotes the sample size and χ represents either the significant wave height, H_{m0} or the mean wave period, T_{m02} computed from the spectral moment $m_n = \iint \sigma^n E(\sigma, \theta) d\sigma d\theta$ (i.e., $H_{m0} = 4\sqrt{m_0}$ and $T_{m02} = 2\pi\sqrt{m_0 m_2^{-1}}$). The subscripts *comp.* and *obs.* refer to the computed and observed values, respectively.

From the scatter indices for H_{m0} and T_{m02} , the optimal calibration coefficients for the OCA model were found to be $\alpha_{LTA}^{OCA} = 0.04$ and $\alpha_{SPB}^{OCA} = 0.07$ with an averaged scatter index of $\overline{s.i.} = 5\%$ and $\overline{s.i.} = 8\%$, respectively. These low α values are consistent with previous studies (e.g. Booij et al., 1999 and van der Westhuysen, 2007). However, they are small compared to the original calibration values of Eldeberky (1996) and Becq-Girard et al. (1999), i.e., $\alpha = 1$. Using the CCA implementation, optimal values closer to $\alpha = 1$ are found with $\alpha_{LTA}^{CCA} = 0.52$ ($\overline{s.i.} = 5\%$) and $\alpha_{SPB}^{CCA} = 0.87$ ($\overline{s.i.} = 8\%$).

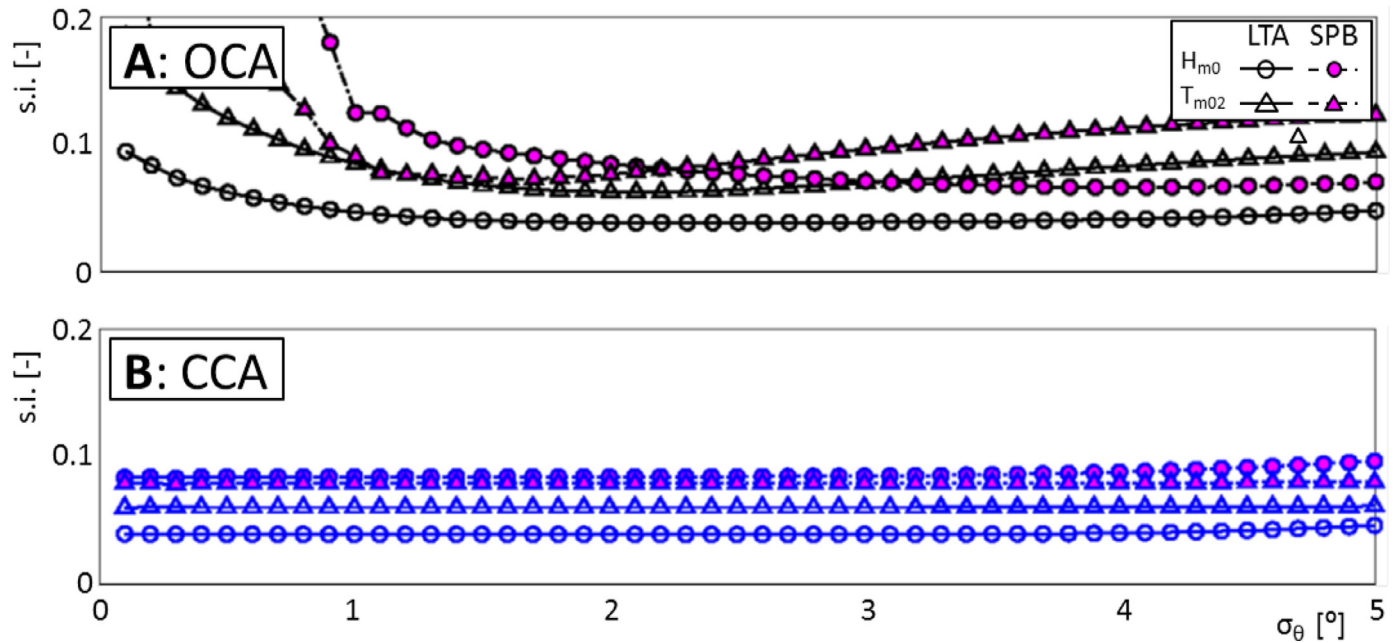


Fig. 4. Scatter indices for the computed H_{m0} (\circ) and T_{m02} (Δ), averaged over the Beji and Battjes (1993) data set and all cases from the Boers (1996) data sets for OCA and CCA models (Panels A and B, respectively).

Using the calibrated model values, we consider the influence of changing the directional aperture of the incident spectra between $0.1^\circ \leq \sigma_\theta \leq 5^\circ$ (Fig. 4). From the scatter index, it is seen that the CCA implementation (Fig. 4B) is insensitive to the directional width of the incident wave spectrum for $\sigma_\theta \leq 4^\circ$, and appears to converge to the unidirectional limit, which is consistent with what we would expect on physical grounds. In contrast, the scatter index for the OCA implementation (Fig. 4A) shows a strong sensitivity to the directional width of the incident spectrum. In particular, as the unidirectional limit is reached, the OCA errors increase significantly, consistent with what was seen in Fig. 1.

4.2. Sensitivity to directional spreading

For the idealized directional cases considered, error characteristics for T_{m02} are shown in Fig. 5. While these results demonstrate a decrease in modeling performance with increased σ_θ , which is likely caused by the models' inability to account for the non-collinear interactions, there is a clear reduction of error between the OCA (blue lines) and the CCA (black lines) for directional wave conditions. For the conditions shown, with $\sigma_\theta \geq 4^\circ$, the typical error in the CCA simulations, for both LTA and SPB models, is less than 50% of the errors in the OCA simulations. The errors for H_{m0} (not shown) are significantly smaller with $\overline{s.i.} \approx 6\%$ and less variability in errors between the directional cases ($\overline{\Delta s.i.} \approx 3\%$). This is consistent with the fact that triad interactions redistribute energy, thus primarily affect the spectral shape, to which T_{m02} is very sensitive.

To further investigate these differences, the computed spectra for Case A with $\sigma_\theta = 30^\circ$ are presented for three locations in the first row of Fig. 6 (Panels A-C). At Station 2, negligible differences between the two model variants occur (OCA; black lines and CCA; blue lines) and overall both are in good agreement with the deterministic model (dashed red lines) irrespective of the choice of triad model (LTA or SPB). However, as the waves propagate into shallower water and the influence of the triad interactions becomes stronger, the differences become more apparent. At Station 6, just

outside the surf zone, the OCA (coupled to either the LTA or SPB) generally underestimates energy transfers. This underestimation of energy transfers in the OCA particularly affects the higher frequencies, i.e., $ff/p \geq 4$ and results in an underestimation of the high-frequency tail by an order of magnitude. At Station 10, which is deep inside the surf zone, this effect is further enhanced. In contrast, with the CCA both triad models perform much better. In particular when combined with the SPB, the overall agreement with the Monte Carlo simulations is excellent.

The more narrow-banded incident spectrum of Case B shows well-defined harmonic peaks in the Monte Carlo simulations at Station 2 and Station 6 (Fig. 6D-F; second row). By Station 10, the high-frequency tail is again largely featureless due to the continued action of the triad interactions (Smith and Vincent, 1992). As in Case A, the OCA models transfer insufficient energy to the higher frequencies, whereas the CCA models predict significant amplification of energy, in better agreement with the Monte Carlo simulations. In particular when coupled with the SPB, the CCA reproduces both the harmonic generation and the eventual development into a featureless tail very well, and is in good quantitative agreement with the Monte Carlo simulations. In contrast, the CCA combined with the LTA cannot reproduce the enhanced energy levels at the non-self-self interaction frequencies (e.g. at $3f_p$) nor does it predict the featureless high-frequency tail (e.g. Booij et al., 2009). Furthermore, with the LTA, energy levels at self-self interaction frequencies (e.g. at $4f_p$) are typically overestimated. These discrepancies appear due to fundamental limitations of the LTA to capture these dynamics and are not associated with the collinear approximation.

In any case, the application of the CCA is shown to significantly reduce the total rms-error for T_{m02} for both the LTA and SPB models. When combined with the LTA, the average rms-error for T_{m02} for Case A and B with $\sigma_\theta = 30^\circ$ goes from 26% for the OCA to 18% for the CCA. With the SPB model, this error goes from 36% for the OCA to 7% for the CCA. These error reductions are shown to be at least comparable, if not larger than the error differences between the LTA and SPB triad models themselves (either with OCA or CCA implementation).

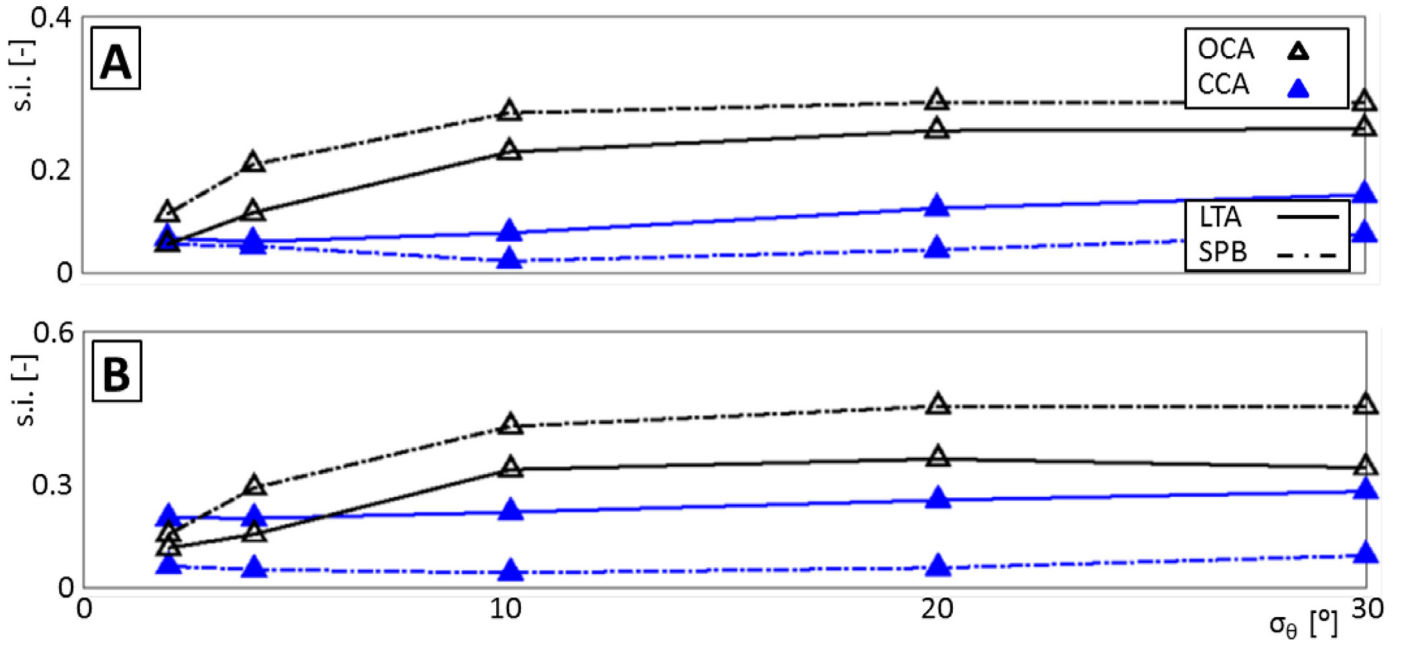


Fig. 5. Scatter index of T_{m02} as a function of directional width for Cases A and B. Comparison is between the OCA (combined with LTA or SPB model) and CCA (with the LTA or SPB model).

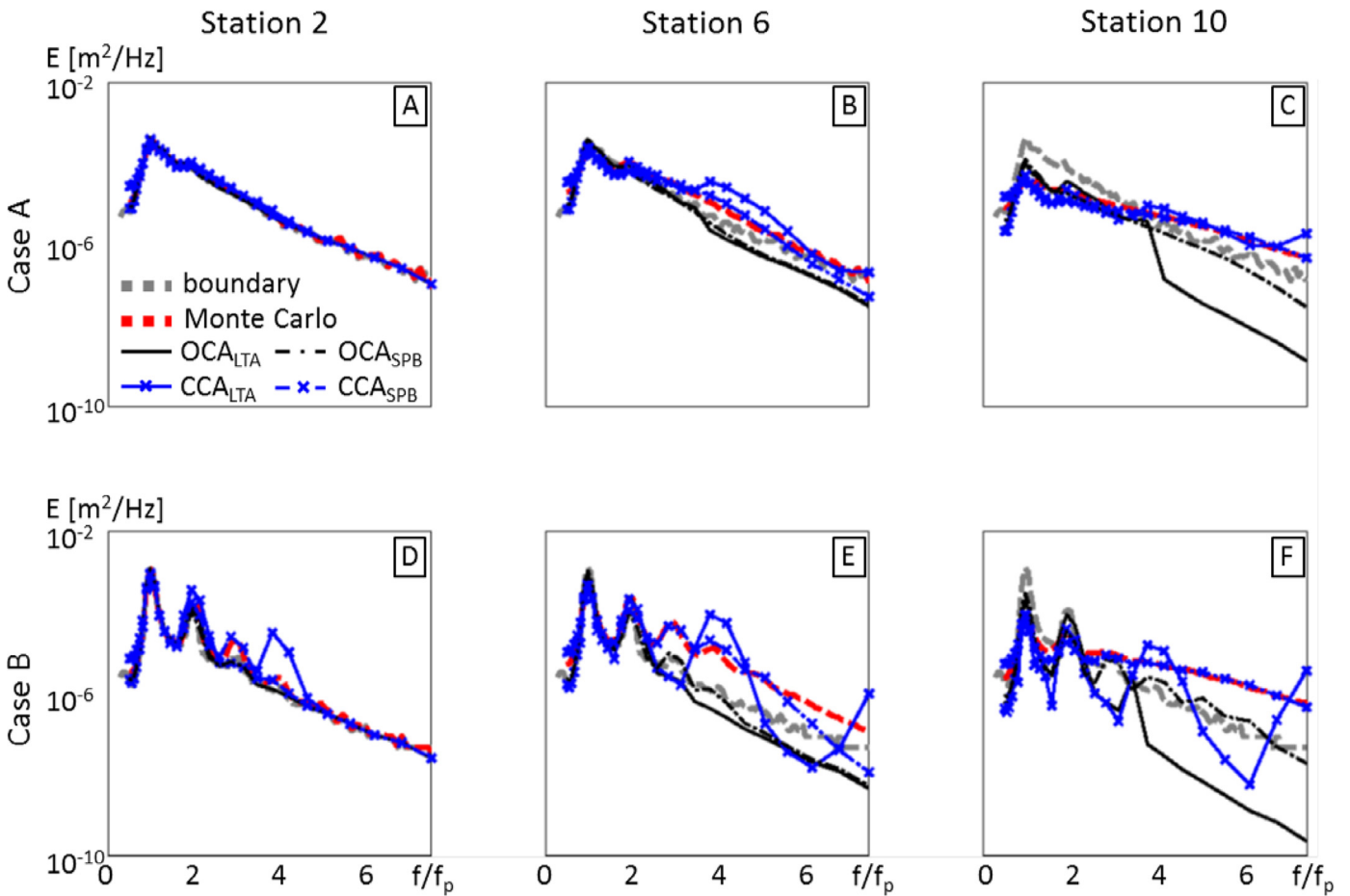


Fig. 6. Variance density spectra for the Case A and B directional wave conditions with $\sigma_\theta = 30^\circ$ at Stations 2, 6 and 10. The gray and red dashed lines represent incident spectra and the Monte Carlo model results, respectively. The spectra computed with the OCA are represented by the black lines and with the CCA in blue with additional (x) markers. The solid and dashed-dotted lines represent spectra computed with the LTA and SPB triad models, respectively. (For interpretation of the references to colour in this figure legend, the reader is referred to the web version of this article.)

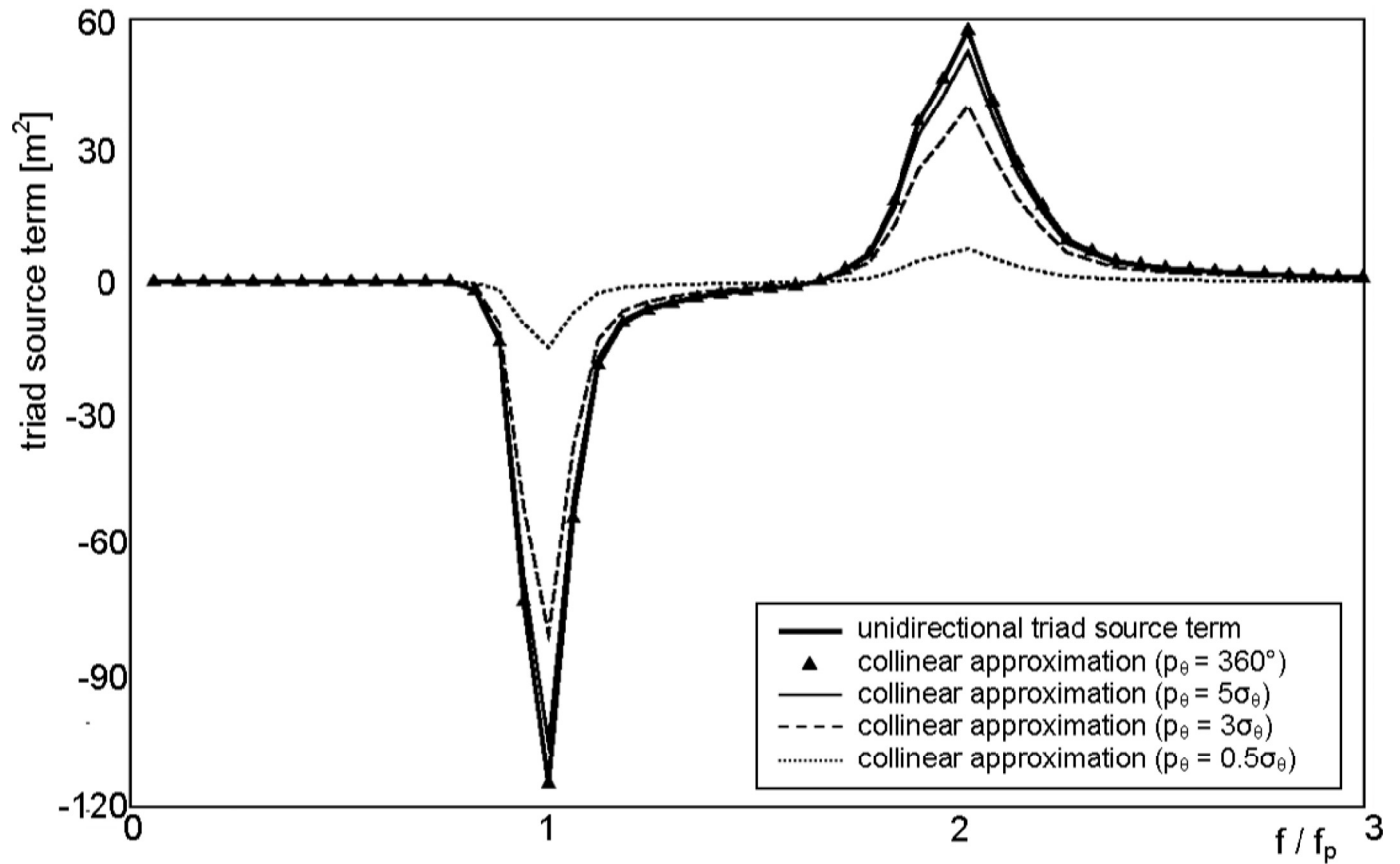


Fig. 7. Energy transfers due to nonlinear triad interactions for a wave field as in Fig. 1 for varying directional bandwidths as computed with the CCA.

5. Discussion

In this study, we revisited the collinear approximations used in operational wave models. We showed that in its conventional form, the OCA can become unbounded resulting in unrealistic transfers of energy away from the spectral peak that results in large errors and potential numerical instabilities. Historically, this inconsistency has mostly gone unnoticed likely because collinear triad models are typically calibrated with flume-type experiments using a fixed, and small, directional distribution with directional spreading, σ_θ^0 (as done here in Section 4.1). As a consequence, the calibration parameter formally becomes a representative angle that is only valid for that particular directional distribution. If the calibrated model is subsequently applied to waves with a different directional spreading, σ_θ (but otherwise identical spectral characteristics), the integrated energy transfers change approximately by a factor $\sigma_\theta^0/\sigma_\theta$. Therefore, for wider directional distributions, the predicted energy transfers rapidly decrease, whereas for narrow distributions, these transfers grow without limit. The net result in operational conditions (where typically $\sigma_\theta > \sigma_\theta^0$) is that these energy transfers are almost always underestimated. While heuristically, one could argue that this is qualitatively reasonable since we would expect lower transfers in short-crested seas, this result relies on a completely arbitrary directional spreading σ_θ^0 used to represent unidirectional conditions with which the model was calibrated. Furthermore, in the few cases where the wave field is indeed more narrowly supported (where nonlinear transfers are stronger and important), predicted energy transfers become effectively unbounded, which may produce unphysical results, and possibly introduces numerical stability issues. For these reasons, a formulation that is internally consistent, reduces to the correct lim-

its for narrow-band wave fields, always produces bound results, and for which we have, through p_θ , some degree of control over how strongly the interactions attenuate with increased directional spreading, is much to be preferred.

In this work, to focus our discussion, we used $p_\theta = 360^\circ$ for all numerical simulations. In this case the integrated energies (Eq. 13) are determined by computing the full directional integral over the energy spectrum. The fact that this gives reasonable results is encouraging as the assumption $p_\theta = 360^\circ$ is actually the least compatible with the collinear assumption on which the approximation is based. The principal effect of p_θ is to reduce the strength of the energy transfers. For instance, using a similar setup as Fig. 1, we see that by reducing p_θ we have some control on the strength of the interaction (Fig. 7).

To assess the sensitivity and robustness of the proposed collinear approximation to p_θ we present the scatter indices normalized by the full directional integral equivalent for Case B with $\sigma_\theta = 2^\circ, 10^\circ$ and 30° in Fig. 8. For all three wave conditions the normalized scatter index asymptotes to unity for $p_\theta \gg \sigma_\theta$ and convergence to the full integral is mostly found for $p_\theta \approx 3\sigma_\theta$ in agreement with Fig. 7. A notable exception is found for $\sigma_\theta = 30^\circ$ where smaller scatter indices are found for lower values of p_θ . This suggests that the use of the full directional integral, in very short-crested seas may lead to some overestimation of the energy transfers (which are small to begin with). The increased scatter index for T_{m02} for smaller values of p_θ is counterintuitive since we would anticipate that results should improve (albeit possibly slightly) for more realistic values for p_θ . This effect is due to an overestimation of T_{m02} due to the insufficient transfer of energy to the higher frequencies.

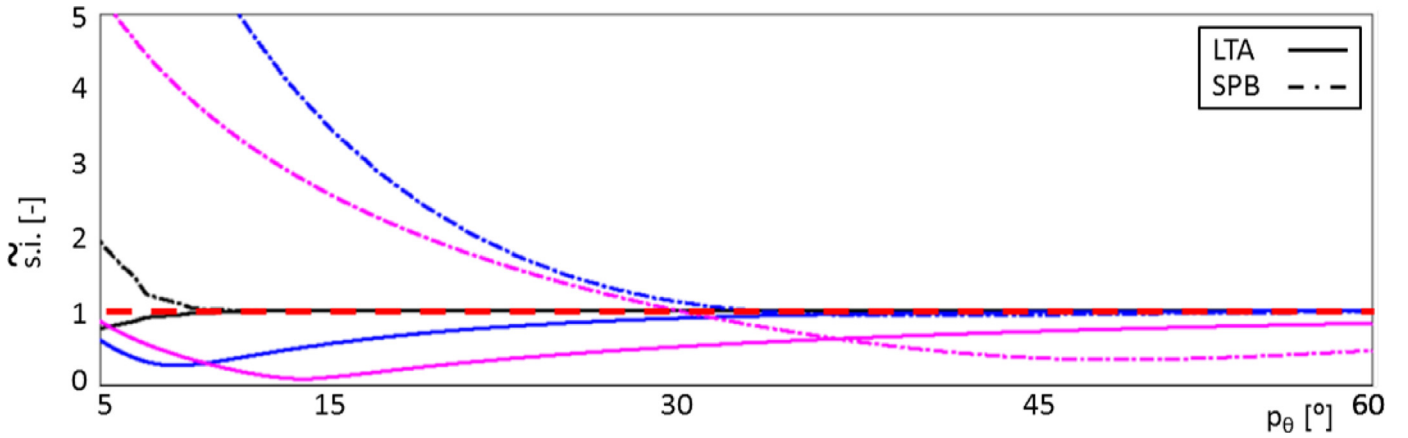


Fig. 8. Sensitivity of the CCA to the directional integration bandwidth p_θ for Case B for varying σ_θ (2° , black; 10° , blue and 30° , magenta). The vertical axis represents the scatter index normalized with the scatter index with the full directional integral. The horizontal dashed red line indicates unity. (For interpretation of the references to colour in this figure legend, the reader is referred to the web version of this article.)

In this work, we set out to identify the source of the unrealistic behavior of the triad source terms when using the OCA to increase the computational efficiency when coupled to the LTA or a different triad model. We propose an alternative collinear formulation (CCA) and compare results for the CCA coupled to two different triad models (LTA and SPB). However, the optimum choice of triad model is clearly outside the scope of this paper. Our objective is to identify the source of the unrealistic behavior of triad source terms when used together with the OCA to increase the computational efficiency. Clearly, the overall quality of the model will greatly depend on the underlying triad model to which the CCA is coupled. The use of any collinear approximation (such as the CCA), and the implied decoupling of non-collinear components remains an admittedly crude approximation driven primarily by the need for efficiency in operational wave models. Possibly, with the improvements proposed here, we can make these collinear models more useful for operational models, and allow larger-scale models to capture some of the principal nonlinear shallow-water effects at reasonable computational cost.

6. Conclusions

In this study, we consider collinear approximations used in operational wave models to compute the nonlinear source term for three-wave interactions for directional wave fields by eliminating the interactions between non-collinear wave components. We demonstrate that the Original Collinear Approximation (OCA), which is presently used in operational wave models (e.g. SWAN), severely overestimates energy transfers in the unidirectional limit (where energy transfers in that approximation become unbounded). At the same time, the OCA underestimates energy transfers in short-crested seas. We propose a Consistent Collinear Approximation (CCA) which has the proper asymptotic behavior in the unidirectional limit and remains well-behaved for wave fields with a wider directional aperture. Comparisons with flume experiments demonstrate that the CCA is a significant improvement over the OCA, is more robust and performs much better overall. Comparisons of the CCA model to Monte Carlo simulations show a significant improvement in overall performance over the OCA. Further improvements are expected through improvements to the underlying triad model.

Acknowledgements

This research is supported by the U.S. Office of Naval Research (Littoral Geosciences and Optics Program and Physical Oceanog-

raphy Program), the National Oceanographic Partnership Program, and the National Science Foundation (Physical Oceanography Program). The first author (James Salmon) is financially supported by the US Office of Naval Research under Grant N00014-10-1-0453 and Grant N00014-12-1-0534. The first author also thanks the Environmental Fluid Mechanics section of Delft University of Technology for additional financial support.

APPENDIX A. Collinear versions of the LTA and SPB models

The collinear approximations discussed in the main text take the form (repeated for convenience)

$$S_{nl3}(\sigma_1, \theta_1) = 2c_{g,1} \left[\int_0^{\sigma_1} W_{2,1-2} \overline{B_{2,1-2}^1} d\sigma_2 - 2 \int_0^\infty W_{2,1} \overline{B_{2,1}^1} d\sigma_2 \right] \quad (A1)$$

where the first integral term represents the sum interactions ($\sigma_2, \sigma_1 - \sigma_2$) and the second the difference interactions ($\sigma_2, \sigma_1 + \sigma_2$). The OCA and CCA are then obtained using the corresponding estimates for the bispectrum

$$\overline{B_{2,1-2}^1(OCA)} = \alpha \Phi_{2,1-2}^1 Q_{2,1-2}^1 \quad \overline{B_{2,1-2}^1(CCA)} = \alpha \Phi_{2,1-2}^1 \overline{Q_{2,1-2}^1} \quad (A2)$$

with $Q_{2,1-2}^1$ and $\overline{Q_{2,1-2}^1}$ defined as in Eqs. (9) and (12), respectively.

The LTA model expresses the imaginary part of the bispectrum in terms of its magnitude and phase (Kim and Powers, 1979) and uses a parameterization for the biphase φ using the spectrally-based Ursell number (Doering and Bouwen, 1995; Eldeberky, 1996; his Eq. 3.19) to control the magnitude of the energy transfers. The quasi-normal closure then takes the form

$$\Phi_{2,1-2}^{LTA} = \frac{\sin |\varphi_{Ur}|}{\Delta k_{2,1-2}} \quad (A3)$$

where $\Delta k_{2,1-2} = k_1 - k_2 - k_{1-2}$ represents the wave number mismatch. To further reduce the computational costs of the integrals in Eq. (A1), the LTA model makes the following additional simplifications. First, it is assumed that the coupling coefficients are equivalent, i.e., $W_{2,1-2} = W_{1,-2} = W_{1,2-1}$ in the expressions for $Q_{2,1-2}^1$ and $\overline{Q_{2,1-2}^1}$. Secondly, the integrals are approximated by the product of a representative value of the integrand, taken to be the self-interactions and an effective frequency interaction bandwidth $\delta\sigma$. Applying this approximation and arguing that $\delta\sigma$ and Δk scale with σ_1 and k_1 , using the notation $\sigma_2 = \sigma_1/2$ for convenience, the CCA version of the LTA is given as

$$S_{LTA}(\sigma_1, \theta) = 2\pi \alpha_{LTA} c_{g,1} c_1 \sin |\varphi_{Ur}| \left[W_{2,2} \overline{Q_{2,2}^1} - 2W_{1,1} \overline{Q_{1,1}^1} \right]. \quad (A4)$$

The OCA version of the LTA is obtained by replacing \bar{Q} with Q in Eq. (A4).

The SPB model of Becq-Girard et al. (1999) assumes a closure approximation based on Holloway and Hendershott (1977). In this case the closure factor takes the form

$$\Phi_{2,1-2}^{SPB} = \frac{\mu}{(\Delta k_{2,1-2})^2 + \mu^2} \quad (\text{A5})$$

where μ represents a proportionality constant between the bispectrum and the fourth-order cumulant. In the SPB model, $\mu = 0.95k_{p,0} - 0.75$, a dimensional parameter where $k_{p,0}$ is the deep water peak wave number. For application in a 2D wave model, where the offshore region is not well defined, we replace the deep water peak wave number with the local peak wave number, k_p . The CCA version of the SPB may then be expressed as

$$S_{SPB}(\sigma_1, \theta) = 8\pi \alpha_{SPB} c_{g,1} \mu \left[\int_0^{\sigma_1} W_{2,1-2} \frac{\overline{Q_{2,1-2}^2}}{(\Delta k_{2,1-2})^2 + \mu^2} d\sigma_2 - 2 \int_0^\infty W_{2,1} \frac{\overline{Q_{2,1}^2}}{(\Delta k_{2,1})^2 + \mu^2} d\sigma_2 \right] \quad (\text{A6})$$

As with Eq. (A4), the OCA version of the SPB is obtained by replacing \bar{Q} with Q in Eq. (A6).

References

- Battjes, J.A., Janssen, J.P.F.M., 1978. Energy loss and set-up due to breaking of random waves. In: Proc. 16th Int. Conf. Coastal Eng. ASCE, Hamburg, pp. 569–587.
- Becq, F., Benoit, M., Forget, P., 1998. Numerical simulations of directionally spread shoaling surface gravity waves. In: Proc. 26th Int. Conf. Coastal Eng. ASCE, Copenhagen, pp. 523–536.
- Becq-Girard, F., Forget, P., Benoit, M., 1999. Non-linear propagation of unidirectional wave fields over varying topography. *Coast. Eng.* 38, 91–113.
- Beji, S., Battjes, J.A., 1993. Experimental investigation of wave propagation over a bar. *Coast. Eng.* 19, 151–162.
- Boers, M., 1996. Simulations of a surf zone with a barred beach, report 1: wave heights and wave breaking. *Commun. Hydraul. Geotech. Eng.* 69 (5), 116.
- Booij, N., Holthuijsen, L.H., Béni, M.P., 2009. A distributed collinear triad approximation in SWAN. *Coast. Dyn.* 2009, 1–10.
- Booij, N., Ris, R.C., Holthuijsen, L.H., 1999. A third-generation wave model for coastal regions. Part I: model description and validation. *J. Geophys. Res.* 104 (C4), 7649–7666.
- Doering, J.R.C., Bowen, A.J., 1995. Parameterization of orbital velocity asymmetries of shoaling and breaking using bispectral analysis. *Coast. Eng.* 26, 15–33.
- Eldeberky, Y., 1996. *Nonlinear Transformation of Wave Spectra in the Nearshore Zone*. Delft University of Technology, Department of Civil Engineering, The Netherlands, p. 203.
- Groeneweg, J., van Gent, M., van Nieuwkoop, J., Toledo, Y., 2015. Wave propagation into complex coastal systems and the role of nonlinear interactions. *J. Wat. Port Coast. Ocean Eng.* 141 (5). doi:10.1061/(ASCE)WW.1943-5460.0000300.
- Hasselmann, K., 1962. On the non-linear energy transfer in a gravity-wave spectrum. *J. Fluid Mech.* 12, 481–500.
- Herbers, T.H.C., Burton, M.C., 1997. Nonlinear shoaling of directionally spread waves on a beach. *J. Geophys. Res.* 102 (C9), 21101–21114.
- Herbers, T.H.C., Elgar, S., Guza, R.T., Guza, R.T., 1995. Generation and propagation of infragravity waves. *J. Geophys. Res.* 100 (C12), 24863–24872.
- Herbers, T.H.C., Orzech, M., Elgar, S., Guza, R.T., 2003. Shoaling transformation of wave frequency-directional spectra. *J. Geophys. Res.* 108 (C1). doi:10.1175/1520-0485(1995)025(1063:IFHMOT)2.0.CO;2.
- Herbers, T.H.C., Russnogle, N.R., Elgar, S., 2000. Spectral energy balance of breaking waves within the surf zone. *J. Phys. Oceanogr.* 30 (11), 2723–2737.
- Hoefel, F., Elgar, S., 2003. Wave-induced sediment transport and sandbar migration. *Science* 229, 1885–1887.
- Holloway, G., Hendershott, M.C., 1977. Stochastic closure for nonlinear Rossby waves. *J. Fluid Mech.* 82, 747–765.
- Janssen, T.T., 2006. *Nonlinear Surface Waves Over Topography*. Delft University of Technology (Library Repository), p. 208.
- Janssen, T.T., Herbers, T.H.C., Battjes, J.A., 2006. Generalized evolution equations for nonlinear surface gravity waves over two-dimensional topography. *J. Fluid Mech.* 552, 393–418.
- Kaihatu, J.M., Kirby, J.T., 1995. Nonlinear transformation of waves in finite water depth. *Phys. Fluids* 7 (8), 1903–1914.
- Kim, Y.C., Powers, E.J., 1979. Digital bispectral analysis and its application to nonlinear wave interactions. *Trans. Plasma Sci.* 7 (2), 120–131.
- Komen, G.J., Cavaleri, L., Donelan, M., Hasselmann, K., Hasselmann, S., Janssen, P.A.E.M., 1994. *Dynamics and Modelling of Ocean Waves*. Cambridge University Press, Cambridge, p. 532.
- Kuik, A.J., van Vledder, G.Ph., Holthuijsen, L.H., 1988. A method for the routine analysis of pitch-and-roll buoy wave data. *J. Phys. Oceanogr.* 18 (7), 1020–1034.
- Madsen, P.A., Sørensen, O.R., 1993. Bound waves and triad interactions in shallow water. *Ocean Eng.* 20 (4), 359–388.
- Orszag, S.A., 1974. *Lectures on the Statistical Theory of Turbulence*. Flow research report 31. MIT, p. 216.
- Smit, P.B., Janssen, T.T., 2016. The evolution of nonlinear wave statistics through a variable medium. *J. Phys. Oceanogr.* 46 (2), 621–634. doi:10.1175/JPO-D-15-0146.1.
- Smit, P.B., Janssen, T.T., Holthuijsen, L.H., Smith, J.M., 2014. Non-hydrostatic modeling of surf zone wave dynamics. *Coast. Eng.* 83, 36–48.
- Smith, J.M., 2004. Shallow-water spectral shapes. In: 29th Int. Conf. Coastal Eng. World Scientific, pp. 206–217.
- Smith, J.M., Vincent, C.L., 1992. Shoaling and decay of two wave trains on a beach. *J. Wat. Port Coast. Ocean Eng.* 118, 517–533.
- Toledo, Y., 2013. The oblique parabolic equation model for linear and nonlinear wave shoaling. *J. Fluid Mech.* 715, 103–133.
- Toledo, Y., Agnon, Y., 2012. Stochastic evolution equations with localized nonlinear shoaling coefficients. *Eur. J. Mech. B/Fluids* 34, 13–18.
- Tolman, H.L., 1990. *Wind Wave Propagation in Tidal Seas*. Delft University of Technology (Library Repository), p. 195.
- Van der Westhuysen, A.J., 2007. *Advances in the Spectral Modelling of Wind Waves in the Nearshore*. Delft University of Technology, p. 207.
- WAMDI group, 13 authors, 1988. The WAM model - a third generation ocean wave prediction model. *J. Phys. Oceanogr.* 18 (12), 1775–1810.
- Zijlema, M., van der Westhuysen, A.J., 2005. On the convergence behaviour and numerical accuracy in stationary SWAN simulations of nearshore wind wave spectra. *Coast. Eng.* 52, 237–256.
- Zijlema, M., van Vledder, G.Ph., Holthuijsen, L.H., 2012. Bottom friction and wind drag for spectral wave models. *Coast. Eng.* 65, 19–26.